The Journal of Neuroscience, May 15, 1999, *19*(10):4090–4101

Reactivation of Hippocampal Cell Assemblies: Effects of Behavioral State, Experience, and EEG Dynamics

Hemant S. Kudrimoti, Carol A. Barnes, and Bruce L. McNaughton

Arizona Research Laboratories-Neural Systems Memory and Aging, University of Arizona, Tucson, Arizona 85724

During slow wave sleep (SWS), traces of neuronal activity patterns from preceding behavior can be observed in rat hippocampus and neocortex. The spontaneous reactivation of these patterns is manifested as the reinstatement of the distribution of pairwise firing-rate correlations within a population of simultaneously recorded neurons. The effects of behavioral state [quiet wakefulness, SWS, and rapid eye movement (REM)], interactions between two successive spatial experiences, and global modulation during 200 Hz electroencephalographic (EEG) "ripples" on pattern reinstatement were studied in CA1 pyramidal cell population recordings. Pairwise firing-rate correlations during often repeated experiences accounted for a significant proportion of the variance in these interactions in subsequent SWS or quiet wakefulness and, to a lesser degree, during SWS before the experience on a given day. The latter effect was absent for novel experiences, suggesting that a persistent memory trace develops with experience. Pattern reinstatement was strongest during sharp wave–ripple oscillations, suggesting that these events may reflect system convergence onto attractor states corresponding to previous experiences. When two different experiences occurred in succession, the statistically independent effects of both were evident in subsequent SWS. Thus, the patterns of neural activity reemerge spontaneously, and in an interleaved manner, and do not necessarily reflect persistence of an active memory (i.e., reverberation). Firing-rate correlations during REM sleep were not related to the preceding familiar experience, possibly as a consequence of trace decay during the intervening SWS. REM episodes also did not detectably influence the correlation structure in subsequent SWS, suggesting a lack of strengthening of memory traces during REM sleep, at least in the case of familiar experiences.

Key words: hippocampus; memory consolidation; sleep; synaptic plasticity; REM; neural ensembles

The hippocampus is thought to play an important role in the acquisition and consolidation of certain forms of memory. Lesions of the hippocampus lead to a temporally graded retrograde amnesia, suggesting that the hippocampus plays a role in the initial encoding of a memory but that, with time, the memory becomes independent of the hippocampus (Scoville and Milner, 1957; McGaugh and Herz, 1972; MacKinnon and Squire, 1989; Kim and Fanselow, 1992; for review, see Zola-Morgan and Squire, 1993; but see Nadel and Moscovitch, 1997). Associative synaptic plasticity (Hebb, 1949) may result in the formation of "cell assemblies" or attractors within the hippocampal formation (Marr, 1971; McNaughton and Morris, 1987; Treves and Rolls, 1994). Although long-term potentiation, a form of artificially induced plasticity, has been demonstrated in the hippocampus and possesses the necessary associative properties (e.g., Bliss and Gardner-Medwin, 1973; Bliss and Lømo, 1973; McNaughton et al., 1978), evidence to show that synaptic connectivity among hippocampal neurons is altered in the course of information storage is mostly indirect.

Rat hippocampal neurons show spatially selective firing (e.g., O'Keefe and Dostrovsky, 1971; Muller and Kubie, 1987; O'Keefe and Speakman, 1987; Quirk et al., 1990; Gothard et al., 1996; Samsonovich and McNaughton, 1997), suggesting a role for the hippocampus in spatial memory encoding. It has been conjectured that firing patterns during behavior may form labile memory traces in the CA3 region of the hippocampus. At the termination of exploration, during states of immobility or sleep, the spontaneous reactivation of these traces may somehow orchestrate the process of memory consolidation in neocortical circuits (Marr, 1971; McNaughton, 1983; Buzsáki, 1989; Chrobak and Buzsáki, 1994; McClelland et al., 1995), possibly by providing a spatial contextual code that serves to bind together the diverse neocortical components of the experience (Nadel et al., 1985; Teyler and Discenna, 1986; McNaughton et al., 1996). This transfer may be facilitated during 200 Hz network oscillations (ripples) in CA1, initiated by synchronized bursts of co-operative CA3 cellular discharge (McNaughton, 1983; Buzsáki, 1986; Wilson and McNaughton, 1994; Ylinen et al., 1995; Shen and McNaughton, 1996).

In support of these ideas, Pavlides and Winson (1989) demonstrated that hippocampal CA1 neurons that were highly active during behavior exhibited increased firing rates during subsequent sleep, relative to previous sleep. At the network level, both the spatial (Wilson and McNaughton, 1994) and temporal (Skaggs and McNaughton, 1996) structures of neuronal firing-rate correlations that appear in a hippocampal neural ensemble during behavior are significantly preserved in subsequent slow wave sleep (SWS), at least for periods of ~30 min. A similar effect is observed in neocortical–hippocampal neuronal-firing interactions (Qin et al., 1997). These results are consistent with the

Received Nov. 30, 1998; revised Feb. 23, 1999; accepted Feb. 24, 1999.

This work was supported by National Institute of Mental Health Grants MH46823 and MH01227 and National Institute on Aging Grant AG12609 and was conducted in partial fulfillment of the requirements for the degree of Doctor in Philosophy (H.S.K.). We thank M. A. Wilson for software support, W. E. Skaggs, S. L. Cowen, M. Tsodyks, T. J. Sejnowski, and A. Treves for useful comments on this manuscript, Jie Wang for assistance with cluster cutting, Casey Stengel and Michael Williams for technical support, and Matt Suster for help with recording.

Correspondence should be addressed to Dr. B. L. McNaughton, ARL-Neural Systems Memory and Aging, 384 Life Sciences North Building, University of Arizona, Tucson, AZ 85724.

hypothesis that there occurs a repetitive broadcast or replay by the hippocampal networks to the neocortex during "off-line" states such as SWS of information acquired during behavior. This replay may constitute an essential element of the process of memory consolidation in the neocortex by a slowly developing synaptic reorganization (McClelland et al., 1995).

The present studies addressed several additional questions about the reactivation phenomenon. Is there a more quantitative statistical estimator of pattern reactivation than the mean correlation measure reported by Wilson and McNaughton (1994), which involved an arbitrary partition of the correlation data into two sets based on their magnitudes? Are the activity patterns in sleep specifically related to the most recent experience, or can multiple experiences be reactivated in the same sleep episode? How persistent is the pattern reactivation phenomenon? Is the strength of reactivation different for novel than for familiar experiences? Given the evidence that rapid eye movement (REM) may play a role in memory consolidation (Fishbein and Gutwein, 1977; McGrath and Cohen, 1978; Bloch et al., 1979; Karni et al., 1994; for review, see Smith, 1995), is there a replay of previous waking patterns during REM sleep? Finally, is the activity during REM related in any way to the previous episode of SWS, and does it have any effect on subsequent episodes?

Parts of this paper have been published previously (Kudrimoti et al., 1995, 1996, 1997).

MATERIALS AND METHODS

Experimental animals

Fourteen adult, male retired-breeder Fischer 344 rats (Charles River Laboratories, Wilmington, MA), with a mean age of 12.5 months at surgery, were at 80% of their weights maintained *ad libitum*. The rats were housed individually and maintained on a reversed 12 hr light/dark cycle throughout the training and recording period. During this time, they had access to water *ad libitum* and were handled and weighed daily. Animal care, surgical procedures, and killing were performed according to National Institutes of Health guidelines for the use of vertebrate animals in research.

Training and recording environments

Eight animals were used in the main experiments. Three wooden tracks were used to train these animals. A triangular track (each side, 75 cm long and 8 cm wide) was used to train three rats. For two of these animals, the same triangular track was used during recording, whereas for the third rat, a linear track (180 cm long and 6 cm wide) was used for the recording sessions. For the remaining five animals, the training and recording environment consisted of a "digital 8"–shaped track (width = 6 cm). This track could be thought of as consisting of two rectangular tracks of dimensions 93 cm × 43 cm with one of the longer sides shared between the two. Tracks with linear configurations were used to ensure repeated sampling of all the locations on the track as the animals performed stereotyped trajectories. During the training and recording sessions, these tracks were placed on a table 1 m from the floor in the center of a moderately illuminated 3.9 m × 3.9 m × 2.5 m room with a black floor, a black ceiling, and multiple visual cues distributed around the perimeter.

Training protocol

Pretraining. Five of the eight rats underwent daily food-rewarded training on linear tracks, 90 cm long, 13 cm wide, and 1 m above the floor, in a different room. The goal of this pretraining was to familiarize the animals with the sequence that they would experience during the training and recording sessions, which consisted of a pre-track epoch (PRE), track running (RUN), and a post-track epoch (POST). Each rat was allowed to sleep or rest quietly in a "nest" for ~30 min (PRE) before the experimenter placed the rat on the track. The rat was then trained to run back and forth along the track, receiving a food reward at both ends (RUN). After ~30 min of track running, the animal was placed back into the nest and allowed to rest for 30 min (POST). The animals learned this task within 1 week and ran on the rectangular digital 8–shaped track during subsequent training and recording sessions. The other three animals did not undergo a formal pretraining protocol; however, they underwent extensive training on the apparatuses on which subsequent recording sessions were performed. All training and recording sessions were performed in the light phase of the animals' diurnal cycle, to maximize sleep duration during recording.

Training. For 1 week after surgical implantation of recording electrodes, the five rats pretrained on the linear track underwent daily food-rewarded training on one-half of the digital 8–shaped track so that they had to traverse a rectangular path. A wooden partition 60 cm high was placed along one side of the long arm of the rectangular track, so that the animal would have visual and physical access only to the one-half of the track on which it was trained. The rat was placed into the nest on the training apparatus and connected to a recording cable. As the rat rested, multiple single-unit and electroencephalographic (EEG) activity was monitored as the electrodes were gradually and intermittently advanced toward the hippocampal CA1 layer. After ~1 hr, the experimenter placed the rat on the track and trained it to traverse the track in a clockwise direction, rewarding it with a mixture of chocolate and rat chow at the two corners farthest away from the partition. After track running, which lasted for 20–30 min, the rat was placed back into its nest and was allowed to sleep for ~1 hr. Two of the remaining three animals were extensively trained (3–4 weeks) to run alternately in clockwise and counterclockwise directions on the triangular track and received "sleep training" before and after track running similar to that given to the other rats. The last animal was trained for 10 d on the triangular track and subsequently on the linear track on which data were collected. Each rat received one training session per day.

Additional animals

Data from an additional six animals, which were prepared, using identical procedures, for different studies, were included in the analysis presented under experiment 2 to confirm the result obtained therein with an independent sample and to increase the sample size in certain analyses. These animals were pretrained on the linear track described above, and then recordings were conducted while they ran for the first and/or second times on either circular, triangular, or rectangular tracks similar if not identical to those described above.

Electrode microdrive construction and surgery

To acquire extracellular spike signals from a large number of single units in parallel and to collect EEG data, a multielectrode microdrive (Wilson and McNaughton, 1993) was implanted unilaterally above the hippocampus of each rat. The methods for the electrode microdrive construction and surgical implantation of the drives have been described in detail by Gothard et al. (1996). Briefly, 14 bundles of four nichrome wire electrodes ["tetrodes" (McNaughton et al., 1983b; O'Keefe and Recce, 1993); total diameter of ~40 μm] were mounted in 14 independent microdrives, such that turning a drive screw allowed manipulation of each tetrode up to a distance of 5–7 mm within a circle 1.5 mm in diameter. The microdrive array was stereotaxically positioned 3.8 mm posterior and 2.5 mm lateral to bregma, above the CA1 region of the hippocampus (Paxinos and Watson, 1982).

Electronics and recording

Twelve of the 14 tetrodes served for unit recording, and the two remaining tetrodes served as reference or EEG electrodes or both. Each electrode within a tetrode was connected to an independent, unity-gain field effect transistor preamplifier. The outputs of the preamplifiers were fed via a multiwire cable to a 64 channel commutator and then amplified (× 10,000) and bandpass filtered (600 Hz to 6 kHz), before being fed into analog-to-digital converter cards housed in eight 80486 personal computers equipped with programmable 10 kHz time-stamp clocks, giving a resolution of 100 μsec. Signals from each tetrode were sampled at 32 kHz using Advanced Discovery data-acquisition software (DataWave, Longmont, CO), and whenever the amplitude of the signal exceeded a preset voltage threshold, a 1 msec sample of the data was time stamped and stored on disk. Signals from one channel from each of 12 tetrodes (generally including the one placed near the hippocampal fissure) were used to acquire continuous EEG data. These signals were amplified 2000 times, bandpass filtered between 1 and 100 Hz or between 1 Hz and 3 kHz, and then sampled at 200 Hz or 1 kHz, respectively. The 200 Hz–sampled data were used to capture the theta rhythm (6–10 Hz) in the EEG during locomotor behavior (Vanderwolf et al., 1975) and REM sleep (Winson, 1972) and "sharp waves" during SWS (Buzsáki, 1986).

The 1 kHz–sampled data were used to identify 100–200 Hz "ripples" in the EEG during SWS (O'Keefe, 1976; Buzsáki et al., 1992; Ylinen et al., 1995).

Light-emitting diodes (LEDs) mounted on the ends of a 15 cm lightweight aluminum rod affixed to the headstage served as markers for position and head direction during data acquisition. Signals emitted by the LEDs were received by a video camera mounted on the ceiling above the recording apparatus, at a resolution of ~2.3 pixels/cm, and were sampled at 20 frames/sec by a tracking device (Dragon Tracker, Model SA2, Boulder, CO). The rat's behavior could also be observed on a television monitor in the computer room.

Recording protocol

Identification of units. After surgery, 12 of the 14 tetrodes were lowered gradually into the hippocampal CA1 layer over the course of 5–7 d. One of the remaining tetrodes remained fixed in the neocortex near the corpus callosum, serving as a reference electrode, whereas the last tetrode was positioned ~300 μm below the CA1 cell body layer, near the hippocampal fissure, and served as an EEG electrode optimized to record the hippocampal theta rhythm. Proximity to the CA1 cell body layer was identified by the presence of ripple–sharp wave complexes, which reverse polarity ~50 μm below the CA1 layer. The cell body layer itself was characterized by the appearance of multiple complex-spike cells (Ranck, 1973; Fox and Ranck, 1981; McNaughton et al., 1983a).

Sleep scoring. After stable hippocampal cell activity was obtained across at least several tetrodes, the experimenter left the recording room and started data acquisition. Sleep scoring was done using a combination of behavioral and EEG criteria. The experimenter observed the rat's behavioral state on the television monitor, while writing down the EEG state four to five times per minute and concurrently listening to an audio monitor for ripples. Baseline data were collected for 20–60 min (PRE). This period consisted predominantly of "large irregular activity" (LIA, sharp wave–ripple complexes heard on an audio monitor or seen in the EEG; the rat apparently sleeping or falling asleep), SWS (the rat clearly sleeping; but no theta rhythm in the EEG; onset often associated with obvious neocortical spindle activity picked up by the callosal reference electrode), and REM (theta in the hippocampal EEG; the rat sleeping). The animal was then placed on the track, and single-unit and EEG data were acquired (RUN) as the animal traversed the track. After track running, the animal was replaced into its nest, and data were collected for a further 60–180 min (POST) as the animal rested quietly and/or slept. This experimental protocol constituted experiment 1.

After two or three such recording sessions on consecutive days, a different protocol was introduced. After PRE, the animals trained on the rectangular track first ran on the familiar half of the track, as in experiment 1. When the rat was on the central arm, the partition was lifted and placed on the other side of the rat, giving the rat access to the novel half (which also included the central arm). The rat was allowed to traverse the track in the novel configuration. Finally, the original configuration was restored, and the animal ran again on the familiar half. There were no pauses between the three track sessions. The rat was then placed back in the nest as before (POST). This protocol was performed with three issues in mind: (1) to confirm that there were no significant changes in the place field configuration during the first and second traversals on the familiar half of the track, thus establishing that the same cells were recorded during the entire track-running period, (2) to determine whether and how the spatial representations of two different environments were reactivated concurrently in sleep after these experiences, and (3) to determine whether the reactivation after novel environments was qualitatively and/or quantitatively different as compared with familiar ones. Questions 2 and 3 formed the basis for experiment 2. Because the sleep periods before and after the familiar and novel halves of the track were the same, nonspecific effects because of sharp wave–induced dynamics in SWS were controlled for in comparisons between the reactivations for each half. This protocol was repeated on the next day. In general, the protocol used in experiment 2 was considered to be a novel experience for the animal, although it was obviously somewhat less novel on the second day. To confirm that the hippocampal representations of the two halves of the track were different, smoothed firing-rate maps of the neurons with place fields on the two halves were constructed by binning the environments (bin size, 1.7 cm × 1.7 cm) (Skaggs at al., 1993). Correlations were computed between the rate maps to assess similarities in spatial representation.

Off-line data analysis

Cell identification. Single units were isolated on each tetrode using a multidimensional "cluster-cutting" technique (McNaughton et al., 1989; Wilson and McNaughton, 1993). This method uses the relative peak amplitudes of extracellular spikes, from several cells recorded simultaneously on the four closely spaced electrodes within a tetrode, to distinguish between the spike generators (McNaughton et al., 1983b).

An isolated unit was classified as a pyramidal cell if (1) it had fired complex spike bursts during SWS, (2) it had been recorded on the same tetrode with other complex spike cells in the CA1 layer, (3) it had a spike width (peak to trough) of at least 300 μsec, and (4) it had a mean firing rate of <5 Hz during track running. Only those pyramidal cells that were stable across PRE, RUN, and POST were included in the analysis. A pyramidal cell was considered to have significant location-specific firing based on a measure that quantifies the amount of information that the occurrence of a single spike conveys regarding the location of the rat (Skaggs et al., 1993). Thus, spatially active single units were pyramidal cells with significant ($p < 0.01$) spatial specificity (place fields) during track-running behavior. Spatially inactive units were pyramidal cells that did not have place fields on the track and fired very few or no spikes during track running. Theta cells (putative interneurons) were excluded from the analysis.

EEG analysis. EEG analysis served two purposes. First, it allowed a differentiation of sleep states. The experimenter selected two raw EEG traces with the largest overall theta rhythm amplitudes, sampled at 200 Hz and 1 kHz, respectively, and visually inspected each trace from the start to the end of both prebehavior and postbehavior sleep. The sleep-scoring notes were matched with the EEG trace and used in conjunction with the EEG waveform to identify periods of REM activity, LIA and SWS states, and awake theta (AWθ). The start and end times of each of these states were flagged and later used to analyze correlations separately during REM and SWS periods (Fig. 1*A*,*B*). Second, the 1 kHz–sampled EEG traces were used to identify the start and end times of ~200 Hz oscillations (ripples) in the EEG recorded near the pyramidal layer and associated with sharp wave (SPW) activity deeper in the stratum radiatum (Ranck, 1973; O'Keefe and Nadel, 1976; Buzsáki, 1986) (Fig. 1*B*). The traces were digitally bandpass filtered between 100 and 300 Hz, and the times of the ripples were identified by an algorithm that detected a ripple when the amplitude of the filtered EEG crossed a set threshold and remained above the threshold for at least 25 msec. Durations of the ripples and inter-ripple intervals were used in comparing the relative strengths of the pattern reactivation during these periods.

Statistical analysis of firing-rate correlation distributions. The spike trains of n pyramidal neurons in a data set were binned into T (100 msec) intervals to obtain sequences of spike counts ($f_i[t]$). The choice of 100 msec was based on previous studies (Wilson and McNaughton, 1994). To check the robustness of the effects described below, four data sets from four different rats were also analyzed using bin sizes of 50 and 200 msec, with comparable results (data not shown). A Pearson's correlation coefficient (C_{ij}, hereafter referred to as a correlation) was calculated between each pair (ij) of spike rate sequences using the formula:

$$C_{ij} = \frac{1/T \sum_{t=1}^{T} f_i[t] \cdot f_j[t] - \mu_i \cdot \mu_j}{\sigma_i \cdot \sigma_j},$$

where μ_i and σ_i are the mean and SD of $f_i[t]$, respectively (Perkel et al., 1967; Gerstein and Perkel, 1969). Ensemble recording from n neurons over T sampling intervals (e.g., 100 msec in the present analysis) generates an $n \times T$ matrix (Q) in which the rows are spike rate sequences (spike "trains," in the limit of short intervals) and the columns are "population vectors" (McNaughton, 1999). C_{ij} can be defined as the cosine of the angle between two row vectors in Q, after subtracting their respective means. It is a real number between −1 and +1 and is a normalized measure of the tendency of the firing rates of both cells to covary on the time scale in question. When C_{ij} is computed for all neuron pairs, a unique $n \times n$ matrix R of pairwise activity correlations is generated. The present study was designed to assess the similarities of the R matrices over different behavioral epochs. R is symmetric, and hence only the lower diagonal portion of it needs to be considered. In addition, only correlations between cells on different tetrodes were used in the analyses. This eliminated the possibility of spurious overlap because of the incomplete isolation of single units.

Experiences presumably are encoded as population vectors in the n

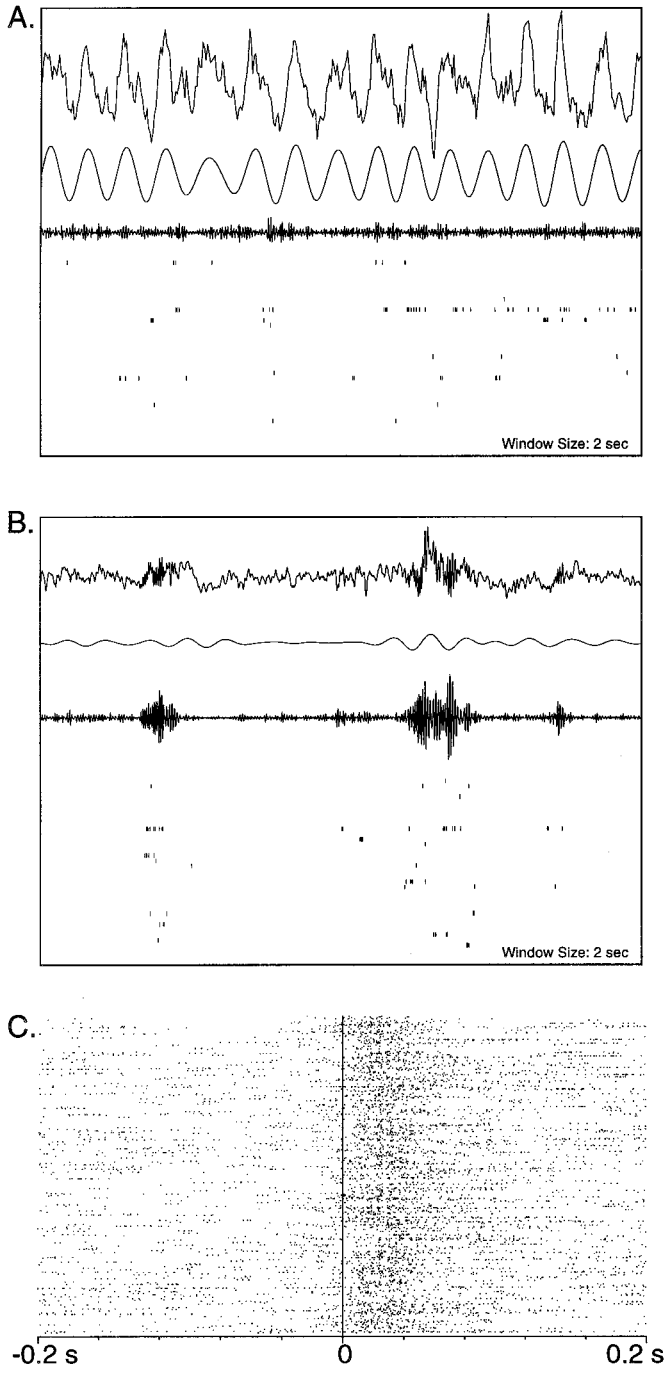

Figure 1. *A*, *B*, EEG traces and concurrent hippocampal single-unit activity during 2 sec periods of REM and SWS in POST. In both *A* and *B*, the *top trace* is the raw EEG waveform acquired by sampling at 200 Hz (*A*) and 1 kHz (*B*). The *second* and *third waveforms* are the EEG data bandpass filtered between 6 and 10 Hz and between 100 and 300 Hz, respectively. In *A*, the 100–300 Hz bandwidth was achieved by filtering the 1 kHz–sampled raw data. At the *bottom* in *A* and *B* are rasters of 36 pyramidal neurons of the CA1 region that fired on the track (not all were active in the time windows shown). Each *vertical tick mark* represents one neuronal action potential, and each *row* of *tick marks* represents the activity of one neuron over 2 sec. Theta rhythm during REM sleep is shown in *A*. The filtered waveform in *A* shows a large 7–8 Hz component compared with that in the corresponding filtered waveform in *B*. The *third waveform* shows very small amplitude 100–300 Hz components in these data. Slow wave sleep is illustrated in *B*. There is an absence of theta modulation in the EEG; however, characteristic large amplitude 200 Hz ripples are clearly observed in the raw data as well as in the 100–300 Hz–filtered waveform. Coincident with the ripples is a burst of activity of the CA1 pyramidal cells, which do not fire in the same manner between ripples. *C*, A raster plot of population activity with respect to ripples. In the figure, 475 ripples occurred in the 10 min epoch of slow wave sleep represented. The start of each ripple oscillation is aligned to the *vertical line* at 0. Each *row* of *tick marks* represents the firing of the population (i.e., it is a combination of spike trains of all of the 36 cells) in a 200 msec window centered around the start of a ripple. It is clearly seen that there is an increase in population discharge during the ripple oscillations, as compared with that in the periods just before the ripples.

dimensional space of neural firing, and a memory trace is presumably a reinstantiation of some approximation of a previously occurring population vector or sequence thereof. The structure of the zero-lag firing-rate correlation matrix R depends entirely and solely on the specific set of population vectors contained in the sample, irrespective of their temporal order (i.e., the state-space occupancy distribution). The assumption made here is that the similarity of the R matrices for two sampling epochs is a reflection of the similarity of the corresponding state-space occupancy distributions (i.e., the similarity of the two sets of population vectors). To the extent that the state-space occupancy distributions differ between two epochs, the R matrices will be less similar. This could occur either because recall is noisy, because different events (i.e., events not in the test set) are being recalled, or because some states are spontaneous and do not reflect recall of any previous input. These cannot be distinguished in the present analysis.

In this approach, it is the relative similarities of correlations and not their magnitudes that are critical. In general, the spread of values in R is expected on statistical grounds to tend toward zero as the number of different population vectors in the sample increases. Thus, correlation magnitudes per se are not of much significance in the assessment of reinstantiation of memory traces. Approximately speaking, the R matrix potentially contains contributions from two sources, one global and one specific to individual cell pairs. Global changes in correlations can arise from any fluctuation or nonstationarity in the net activity of the system over the sampling interval. These could be caused by fast or slow external modulation, for example, changes in circulating hormone levels or in the activity of subcortical inputs such as the septohippocampal GABAergic and cholinergic systems or the median raphe serotonergic system, or by intrinsic dynamics such as intrinsic oscillations, sharp waves, etc. (see Fig. 1*C*). Changes in global modulation may be expected to change the mean values of the correlations, without much change in their relative magnitudes, at least within some range.

The present study was designed to investigate the dynamics of memory trace reactivation during sleep and/or quiet waking. We approach this by quantifying how much of the variance in the elements of R during sleep can be explained (statistically speaking) by their relative magnitudes during a previous active waking experience, after taking into account their relative magnitudes in sleep before the experience. This enables the comparison across time and behavioral state of the effects of previous experience on the microstructure of the firing-rate correlation pattern. The explained variance (EV) of the correlation pattern in sleep (POST), caused by a track-running experience (RUN), was computed using the square of partial correlation coefficients in a multiple correlation analysis (Kleinbaum et al., 1988) in which the lower diagonal elements of the corresponding ensemble firing-rate correlation matrices, for the periods PRE, RUN, and POST, were entered as variables:

$$EV = r^2_{\mathrm{RUN,POST|PRE}} = \left(\frac{r_{\mathrm{RUN,POST}} - r_{\mathrm{RUN,PRE}} r_{\mathrm{POST,PRE}}}{\sqrt{(1 - r^2_{\mathrm{RUN,PRE}})(1 - r^2_{\mathrm{POST,PRE}})}} \right)^2,$$

where $r_{\mathrm{RUN,POST|PRE}}$ reflects the effects of the maze experience (RUN) on the activity correlations in POST, after controlling for any preexisting relationship that might have been present in PRE. The analysis typically used correlations during the last 10 min of baseline SWS (PRE) and track running (RUN) as independent variables and the correlations in three 10 min epochs in postbehavior SWS (POST) as dependent variables. The relationship between RUN and POST correlations was thus measured after controlling for the linear effects of PRE correlations on both of these variables. For experiment 2, the relationship between the activities in the two different halves of the maze was also controlled for, enabling an assessment of the independent contributions of the two experiences to

←

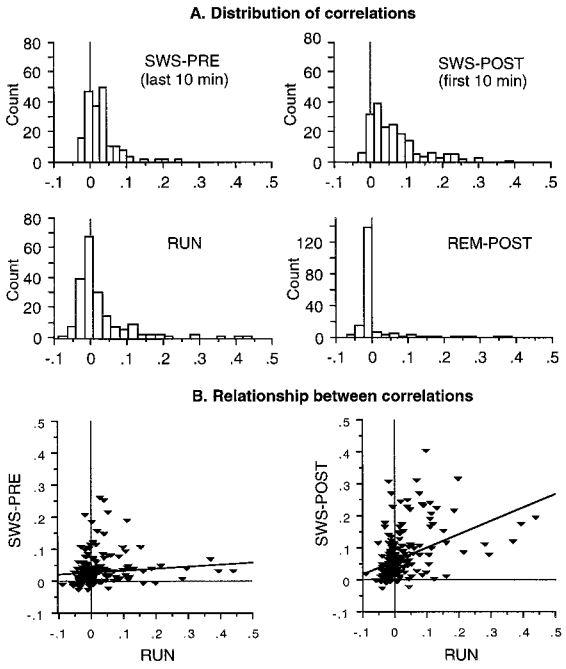

Figure 2. *A*, Example distributions of the pairwise correlations from one recording session (familiar track). Histograms show distributions of correlations during SWS PRE (last 10 min), SWS POST (first 10 min), track-running behavior (RUN), and REM POST. *B*, Data from the same recording session showing the relationship between pairwise correlations during RUN and SWS PRE (*left*) and the relationship between correlations during RUN and SWS POST (*right*). Each data point in the scatterplots corresponds to one cell pair, both members of which had place fields on the track. For illustrative purposes, the relationship between track and sleep correlations has been shown using a simple linear regression fit. In the actual analysis of POST versus RUN, a multiple correlation model that controlled for the effects of PRE was used.

the correlation variance during POST. In sessions in which REM occurred during postbehavior sleep, the correlation during the REM episode was also used as a dependent variable. In some analyses, SWS epochs were parsed into SPW and inter-SPW segments, and the magnitudes of the EV for these two conditions were compared.

A typical example of the distribution of pairwise rate correlations during track-running behavior and during SWS and REM sleep states is shown in Figure 2*A*. An illustrative example of a simple linear regression fit is shown in Figure 2*B*. For the actual RUN–POST comparison, a partial correlation coefficient controlling for the linear effects of PRE on both the variables was used. For the PRE–RUN comparison, a simple correlation coefficient was computed. For illustrative purposes and for comparison with the results of Wilson and McNaughton (1994), some data were sorted into cell pairs that were relatively highly correlated during track running (HICOR) and cell pairs that were relatively uncorrelated during track running (UNCOR) using a cutoff of +0.01. Although this cutoff is arbitrary, it was a reasonably consistent value by which cells with completely or partially overlapping spatial fields could be distinguished from those with nonoverlapping fields. The multiple correlation approach provides a more quantitative estimate of the true strength of trace reactivation because it takes into account all of the variance in the data, rather than partitioning the data arbitrarily into two groups. It also provides a means of estimating explicitly the magnitude of the contribution of recent experience to the correlations, by removing the contributions of preexisting correlation structure in the network. Most statistical analyses were performed using the SPSS (Chicago, IL) statistical package.

To verify that the partial regression analysis was indeed capable of removing the effects of any preexisting similarity between *R* during POST and *R* during RUN, tests were performed in which one-half of the RUN period was substituted for PRE in the analysis of the relationship between the other one-half of the RUN period and POST. As expected, this resulted in an EV for the RUN–POST comparison of ~0.

RESULTS

The results are based on 42 recording sessions from 14 rats. A recording session consisted of data collection during a prebehavior sleep period (PRE), spatial behavior on one or more tracks (RUN), and a postbehavior sleep period (POST). From 16 to 63 pyramidal cells were recorded per session for an average of ~32 cells/session. In this study, a total of 18,051 correlations were computed from 1335 pyramidal cell unit recordings. Although it is likely that some cells were recorded from more than once, most of the results were observed independently in each session.

Mean firing rates and average correlation of the population before and after track running

Using data collected in experiment 1 (highly familiar track), we computed the firing rates of cells during PRE and POST for two cell groups: cells with fields on the track ($n = 423$; mean firing rate during RUN, 1.03 ± 0.03 Hz) and cells inactive on the track ($n = 237$). There was only a slight (nonsignificant) increase in firing rates from PRE to POST of the cells that had fields on the track (Fig. 3*A*; difference of ~14%; $p > 0.05$). Cells that did not fire during behavior also showed no change in their mean firing rates ($p > 0.05$). The small increase in firing rates of the active population decreased rapidly with a time constant of ~20 min. Pairwise correlations between cells on different tetrodes were computed during PRE, RUN, and POST. The mean correlation of the population of cells with fields increased significantly from PRE to POST but rapidly decayed (Fig. 3*B*; $\tau \sim 12$ min). In addition, the correlations during PRE and POST were sorted by whether the cell pairs were coactive, i.e., had overlapping fields during RUN (Fig. 3*C*; $C \geq 0.01$, HICOR), or were active but uncorrelated during RUN ($C < 0.01$, UNCOR). Correlations of the HICOR group increased from PRE to POST but rapidly decayed ($\tau \sim 18$ min). Thus, the behavior-related elevations of firing rates and pairwise correlations decayed rapidly during POST.

Correlation patterns during sleep were partly explained by the patterns during previous track running

A multiple correlation analysis was performed on the activity correlations during RUN, PRE, and POST. There was a significant relationship ($r_{\text{RUN–POST|PRE}}$, $p < 0.0001$) between the correlations during RUN and those during POST after controlling for the linear effects of PRE correlations. These effects were significant in all data sets. The activity patterns of hippocampal pyramidal cells during behavior in a highly familiar environment explained ~15% of the variance in the firing-rate correlations among these cells during sleep immediately after behavior (i.e., Fig. 3*D*; EV = 0.15).

Because the partial coefficient $r_{\text{RUN–POST|PRE}}$ controls for the linear effects of PRE, the baseline level of EV can thus be taken to be 0. Using the 30 min of POST, we fitted an exponential to the decay of EV and obtained a slower time constant of ~30 min (compared with the faster time constants of the firing rates and correlation magnitudes), suggesting that the similarities of the correlations outlast the changes in the overall mean values of the correlations or the changes in firing rates per se.

Correlation patterns during behavior on a familiar track can sometimes be predicted from the patterns during prebehavior sleep

If activity patterns persist in the hippocampus, then, for a familiar experience that is repeated daily, some of the variance in the correlations during PRE should also be explainable by the pattern

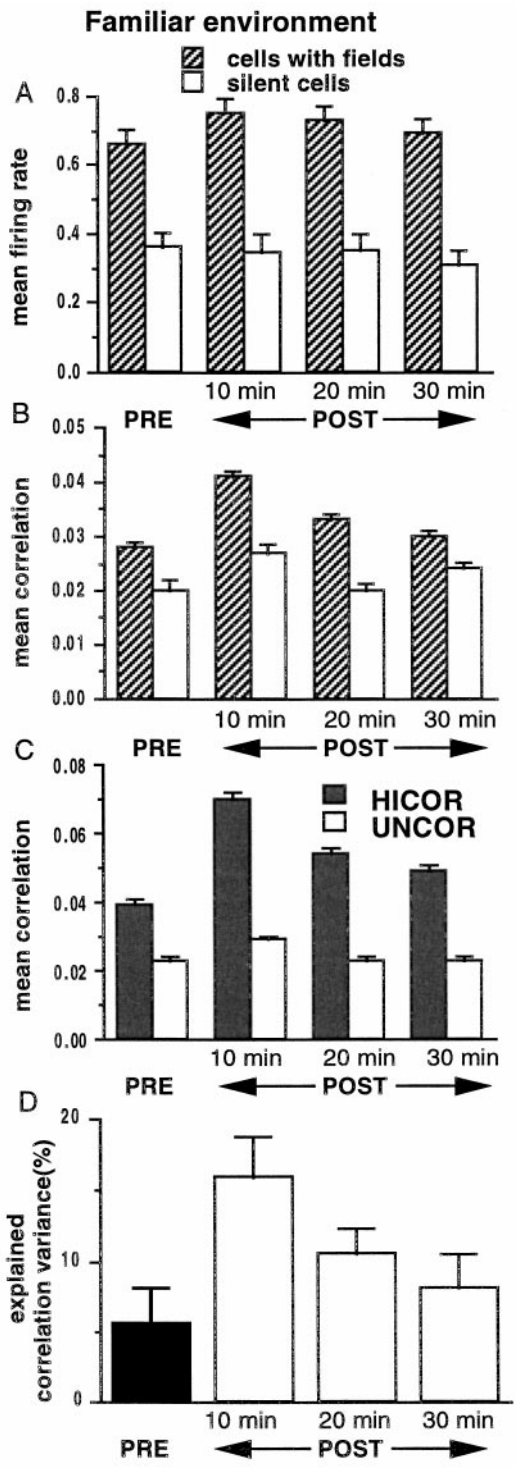

Figure 3. *A*, Histograms of the mean firing rates of pyramidal neurons during pre-behavior SWS (PRE) and three 10 min intervals in post-behavior SWS (POST), computed by averaging across 22 track-running sessions from seven rats, are shown. The firing rates of cells with place fields on the track ($n = 423$) increased marginally ($p > 0.05$, ANOVA) and returned rapidly toward their PRE levels with a time constant of 20 min. For all periods, the firing rates of cells with fields on the track were significantly higher than were the firing rates of cells inactive during track running ($n = 237$; $p < 0.05$, ANOVA). *B*, Mean correlations of cell pairs (using 100 msec bins) during the same time periods described in *A* are shown. The mean correlation of cells active on the track increased from PRE to POST ($p < 0.05$), but the increase rapidly declined over the 30 min period ($\tau = 12$ min). The mean correlations of cells inactive on the track did not change significantly ($p > 0.05$, ANOVA). *C*, In the cell group with fields on the track, correlation values were sorted into HICOR (correlation ≥ 0.01) and UNCOR (correlation < 0.01) sets. The mean correlation of the HICOR set was significantly higher compared with the mean correlation of the UNCOR set ($p < 0.05$, ANOVA). This difference, present in 6 of 22 sessions in PRE, was enhanced in all 22 sessions during POST (significant interaction on a repeated-measure ANOVA) as the mean correlation of the HICOR set (mean correlation of 0.10 ± 0.003 on track) increased from a PRE value of 0.04 ± 0.002 to a POST value of 0.07 ± 0.002 ($p < 0.05$, ANOVA). This increase decayed rapidly ($\tau = 18$ min). The mean correlation of the UNCOR set (mean correlation of -0.02 ± 0.000 on track) increased from a PRE value of 0.02 ± 0.001 to 0.03 ± 0.000 in POST ($p > 0.05$, ANOVA). It is theoretically possible that the differences in the mean correlations between the two groups in the histogram could be attributable to differences in the firing rates of the neurons in the two groups; however, the majority of cells were members of pairs in both groups, and there were no significant differences in the mean firing rates between the HICOR and UNCOR cells during POST (19 of 22 sessions; $p > 0.05$). *D*, Explained correlation variance (EV) during the same time periods described in *A* are shown. For PRE, EV was computed using the square of the simple correlation coefficient $r_{\text{RUN–PRE}}$ (*solid bar* on *left*). For POST, EV was computed using the square of the partial correlation coefficient $r_{\text{RUN–POST|PRE}}$ (3 *bars* on *right*). The EV for all periods of SWS was significantly >0 ($p < 0.001$, ANOVA) and increased significantly after behavior ($p < 0.05$, ANOVA). The decay time constant (baseline = 0) was 30 min, suggesting that the similarity of the correlation matrices for the RUN and POST periods outlasts changes in the average magnitude per se. Note that the baseline for the POST EV is 0, not the PRE value, which is removed by the partial correlation procedure (see Materials and Methods).

during behavior. In all 22 sessions for experiment 1, the environment was already highly familiar. In 6 of these sessions (from three different rats), there was a significant relationship between the RUN correlation structure and that during PRE ($p < 0.00001$ in three sessions; $0.003 \leq p \leq 0.006$ in the other three sessions). In the remaining 16 sessions, $r_{\text{RUN–PRE}}$ was positive, indicating a significant trend. In experiment 2 (see below), PRE effects were seen for the familiar track in two of six data sets, consistent with the proportion seen in experiment 1. Overall, the activity patterns of hippocampal pyramidal cells during behavior in a highly familiar environment accounted for, on average, ~5% of the variance in the coactivity patterns of these cells during sleep immediately before RUN (Fig. 3*D*).

The foregoing PRE effects might reflect residual traces of memory for familiar experiences, lasting at least until the next day. This hypothesis predicts that, for novel environments, there should be no relationship between correlations during PRE and RUN and a possibly weaker relationship between the correlations during RUN and POST as compared with highly familiar experiences. These questions are addressed in experiment 2.

Trace reactivation in SWS occurs most robustly during ripples

During SWS and quiet wakefulness (LIA), pyramidal cells in the hippocampus fire intermittently in synchronized bursts, associated with ~200 Hz ripples near the cell bodies and simultaneous SPW in the stratum radiatum (see Fig. 1). Because ripples were identified on the basis of EEG traces, only those data sets with robust ripple activity in the EEG record (i.e., those with optimal positioning of the EEG electrodes) were considered for analysis of activity during ripples and inter-ripple intervals. Using this criterion, we selected 12 track-running sessions, in which the postbehavior sleep period had 10 min of continuous SWS and/or LIA activity in the first 30 min of sleep. Correlations were

computed separately for spike rates during the ripple periods and during the inter-ripple intervals.

For a set of random variables, the variance of their correlation distribution is inversely proportional to the square of the length of the sampled epoch. Because a major fraction of SWS is spent in the inter-ripple state (mean duration of 1.2 sec for inter-ripple intervals vs 73 msec for ripples), it is necessary to equate the total sampling time for the two states. Therefore, a period in each inter-ripple interval midway between the two ripples bounding it and of duration equal to that of the preceding ripple was selected. The ripple and inter-ripple segments were then pooled for correlation analysis.

Mean firing rates of the population during ripples increased slightly from PRE to POST ($p < 0.05$), but this increase decayed rapidly with a time constant of ~13 min (Fig. 4*A*). Mean correlations during ripples did not change from PRE to POST (Fig. 4*B*). Although the mean firing rates were significantly different ($p < 0.05$, ANOVA) between ripples and inter-ripple intervals, the mean correlations were not different during POST (Fig. 4*B*; $p > 0.05$). The mean ripple duration decreased from PRE to POST (Fig. 4*C*; $p < 0.05$), but the number of ripples increased (Fig. 4*D*; $p < 0.05$). A ripple index, representing a ratio of the total number of spikes emitted during ripples to the number during inter-ripple intervals, increased from PRE to POST, presumably because of the increase in firing rates during ripples (Fig. 4*E*; $p < 0.05$). There was a significant relationship ($r_{\text{RUN–POST|PRE}}$, $p < 0.001$) between the correlations during RUN and those during both ripples and inter-ripple intervals in POST. As shown in the three sets of *bars* on the *right* in Figure 4*F*, the correlations during behavior explained a significant proportion of the correlation variance during ripples and during inter-ripple intervals after the behavior ($p < 0.05$, *t* tests; chance = 0%). During the first 10 min of SWS, EV was significantly higher during ripples than during inter-ripple intervals ($p < 0.05$, ANOVA). The decay time constant for the EV during ripples was 30 min.

Effects of multiple experiences on pattern reactivation

In experiment 2 (2 consecutive days for each of three rats), the animal ran first on the familiar configuration (F1) of the figure-8 track and then on the unfamiliar configuration (N), followed by another session on the original configuration (F2). Because the second configuration was relatively novel on both days, data from both days were considered together. Although the two halves of the track were very similar in shape and alignment with respect to extratrack cues, the place fields of the same cells were mostly different in the two regions. For example, 18 of the 58 cells recorded on the first day of experiment 2 did not have fields on the novel half. For cells that had fields on both halves, the firing-rate map correlations between fields of the same cell had a mean value of 0.30 ± 0.06. For comparison, the corresponding rate map correlations for F1 versus F2 were 0.76 ± 0.02, indicating highly similar fields during two episodes in the familiar environment. On the second day of experiment 2, 17 of 73 neurons with place fields on the familiar half did not fire on the novel half, and the spatial firing patterns between the two halves had a lower correlation (0.17 ± 0.06). Similarly, the temporal activity correlation patterns for the two environments were somewhat correlated ($r = 0.3$ and 0.5 on days 1 and 2, respectively). Some of the correlation between the spatial and temporal activity patterns in the two environments may have been attributable to the fact that the central arm of the track (i.e., approximately one-third of the track) was common to both N and F configurations. In any case, this correlation was controlled for in estimating the independent effects of both halves of the maze during POST. Thus, $r_{\text{N-POST|PRE,F2}}$ was computed for the novel half (N) of the track, and $r_{\text{F2-POST|PRE,N}}$ was computed for the familiar half (F2) for subsequent 10 min intervals in postbehavior sleep as in experiment 1.

The correlation structures for two sequentially visited environments both contributed to the correlation structure in sleep

As in experiment 1, the mean correlations of the population increased from PRE to POST but decayed rapidly with time constants of 36 min (N) and 27 min (F2) on day 1 and with time constants of <10 min on day 2. $r_{\text{N-POST|PRE,F2}}$ and $r_{\text{F2-POST|PRE,N}}$ were significant ($p < 0.001$). In POST, the EV for both N and F2 was above chance (Fig. 5; $p < 0.05$, *t* tests), and the EV for N was significantly smaller than that for F2 (Fig. 5; $p < 0.05$). This was observed in spite of the fact that mean correlations were somewhat higher for N (0.0677 ± 0.002) than for F2 (0.0558 ± 0.002) in the first 10 min of POST ($p < 0.05$) and were not significantly different from those for F2 in all other periods ($p > 0.05$). The combined independent contributions of N and F2 accounted for ~30% of the variance of the correlation distributions during POST. Examination of the ripple dynamics in the manner illustrated in Figure 4 did not reveal any differences between experiments 1 and 2 that might have accounted for the increased EV.

Correlations in PRE did not predict those in RUN for a novel experience

If the significant EV in PRE attributable to RUN and observed in experiment 1 was caused by a memory effect lasting from one day to the next, there should be no such effect for a novel environment. Consistent with this prediction, in experiment 2, $r_{\text{PRE-N|F2}}$ was not significant (data not shown; i.e., there was no significant relationship between the correlation patterns during PRE and RUN for the novel experience in any of the six data sets). Significant PRE effects were seen for the familiar half in two of six data sets, consistent with the proportion seen in experiment 1. The magnitude of the PRE effect for the familiar environment was significantly larger than that for the novel (Wilcoxon signed rank test, $p < 0.043$). To address this issue further using independent data, we compared data from nine recording sessions in a separate experiment, in which six animals ran on entirely novel mazes, with the familiar environment data from experiment 1. There was a significantly larger PRE effect for familiar environments (Mann–Whitney *U* test, $p < 0.005$; mean EV, 5.7 ± 2.7 for familiar and 0.37 ± 0.23 for novel).

Correlation structure during REM

In several recordings, REM sleep was observed in post-behavior sleep (see Fig. 1*A*). In sessions in which POST data were collected for >1 hr, the animals had a few episodes (up to four) of REM sleep (average duration, 1.85 ± 0.17 min). In most of the data sets, however, only one REM episode occurred during POST. To test whether reactivation of activity patterns occurs during REM sleep and whether a REM episode has any relationship with the correlations during the SWS before and after it, we computed correlations between hippocampal pyramidal cell pairs in post-behavior sleep (seven recording sessions from four rats). The data

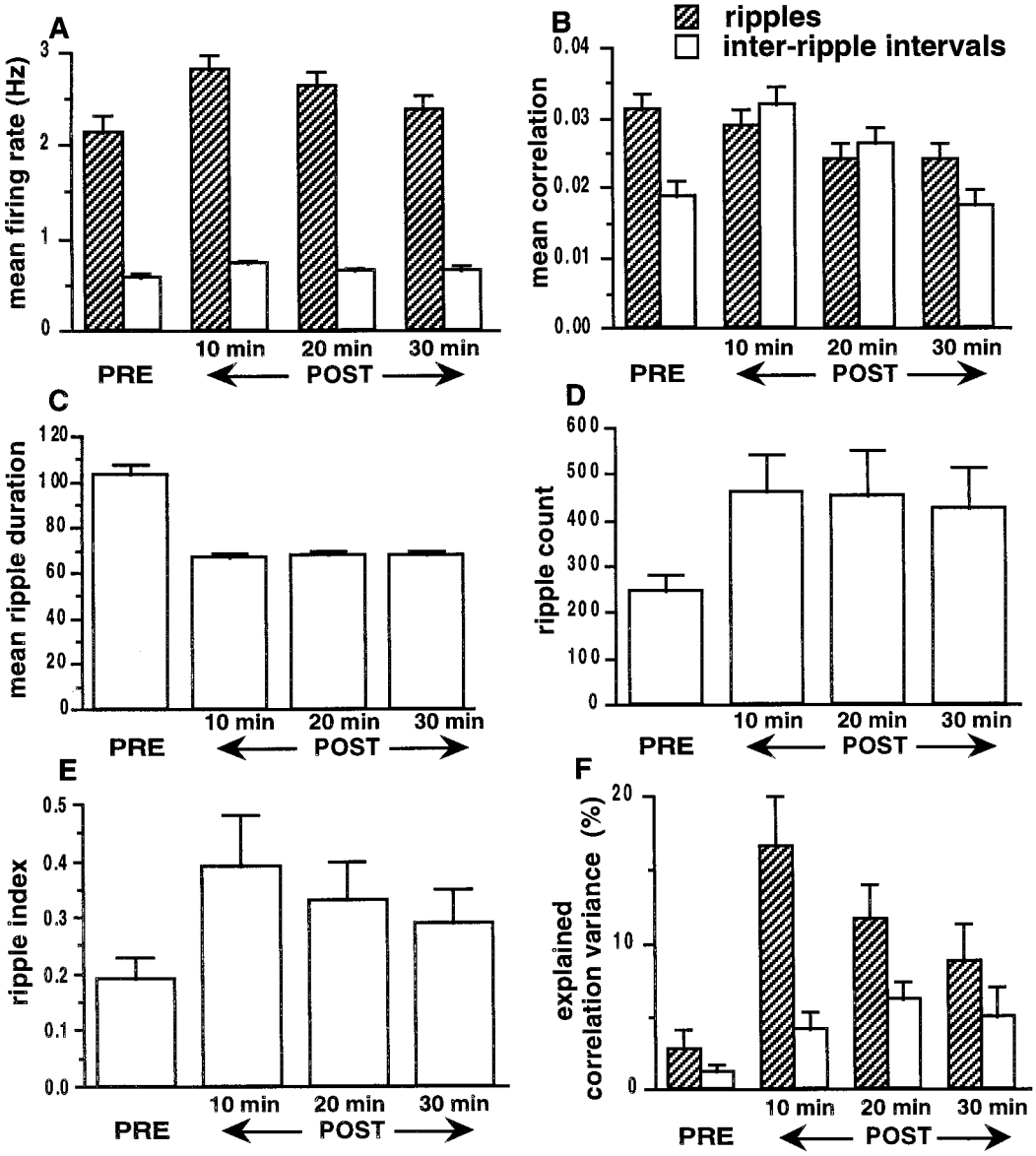

Figure 4. Ripple analysis for a subset of data from experiment 1 (12 recording sessions; familiar environment). *A*, Histograms show the mean firing rates of the population with place fields ($n = 258$), during ripples and during inter-ripple intervals. For all periods, the firing rates during ripples were significantly higher than were the firing rates during inter-ripple intervals of comparable duration ($p < 0.05$). The firing rates during ripples increased from PRE to POST ($p < 0.05$) and decayed over a 30 min period with a time constant of ~13 min. The firing rates during inter-ripple intervals did not change ($p > 0.05$). *B*, During POST, mean correlations during ripples and inter-ripple intervals were not different ($p > 0.05$). The mean correlation of the population during ripples did not change from PRE to POST. The mean correlation during inter-ripple intervals increased from PRE to POST but decayed rapidly ($\tau = 8$ min) to PRE levels. *C*, The average duration of ripples decreased from PRE to POST ($p < 0.05$) but remained constant during the 30 min of SWS in POST ($p > 0.05$). *D*, The number of ripples increased from PRE to POST ($p < 0.05$) but did not decrease significantly over the 30 min interval ($p > 0.05$). *E*, Histograms show a ripple index that was computed as: (percent time in the ripple state × the mean firing rate of the population during ripples)/(percent time in the inter-ripple state × the mean firing rate of the population during inter-ripple intervals). The index increased from PRE to POST ($p < 0.05$), and there was a decreasing trend in POST ($\tau = 28$ min). *F*, For PRE (ripple and inter-ripple periods), EV was computed using the square of the simple correlation coefficient $r_{\mathrm{RUN-PRE}}$ (*bars* on *left*). For POST (ripple and inter-ripple periods), EV was computed using the square of the partial correlation coefficient $r_{\mathrm{RUN-POST|PRE}}$ (3 sets of *bars* on *right*). EV during ripples and inter-ripple intervals in POST was significantly above chance ($p < 0.05$) and increased significantly after behavior ($p < 0.05$, ANOVA). During the first 10 min of SWS, the EV was greater during ripples ($p < 0.05$). The decay time constant for the explained correlation variance during ripples was 30 min. (Note again that the baseline for the POST EV is 0, not the PRE value, which is subtracted by the partial correlation procedure).

were separated into the following epochs (Fig. 6, *top*): a 3 min SWS interval starting 10 min before a REM episode (*block 1*), a 3 min SWS period just before the REM episode (*block 2*), the REM episode (*REM*), and a 3 min SWS interval just after the REM episode (*block 3*). An ANOVA revealed no significant differences ($p > 0.05$) between the mean firing rates in the REM period (mean firing rate, 0.48 ± 0.04 Hz) and in the SWS episodes that preceded (block 2; mean firing rate, 0.61 ± 0.04 Hz) and followed it (block 3; mean firing rate, 0.56 ± 0.05 Hz). Between blocks 1 and 2, there was a decreasing trend in the EV.

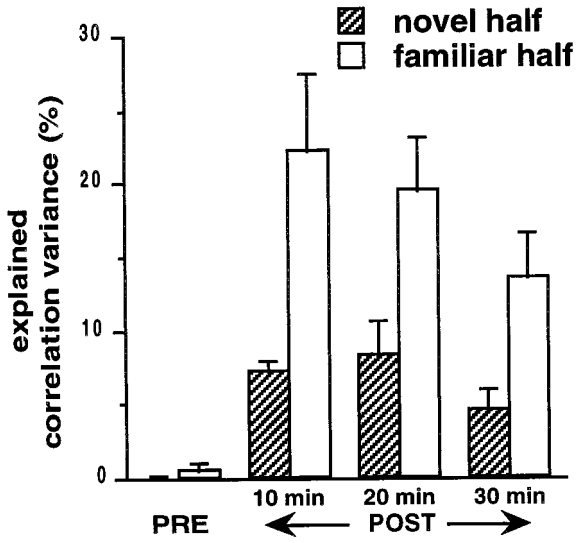

Figure 5. In experiment 2, the animals traversed the familiar half of the digital 8–shaped track first and then ran on the second, novel half of the track before running on the familiar half again. During POST, the independent contributions of both regions to the explained variance (i.e., after controlling for any correlation between regions) were significantly above chance. Also, the EV for the familiar half was significantly above that for the novel half ($p < 0.05$, Mann–Whitney *U* test). For both halves, the explained variance had slower time constants of decay (~43 min), in comparison with that of the familiar-only experiments.

In the familiar-only condition (experiment 1), there was no significant effect of the waking experience on the correlation structure during REM

Although the EV for blocks 1 and 2 of SWS was significantly >0, the EV was not above chance (Fig. 6; $p > 0.05$) for a comparable period of REM immediately after block 2; nor, however, was the EV for the next SWS block different from 0. It is thus not clear whether the lack of significant EV during REM was caused by the ongoing decay of the EV per se or by some intrinsic difference in reactivation dynamics during REM. The mean correlations during the REM episode (0.0095 ± 0.014) were significantly lower than the correlations during SWS (block 1, 0.031 ± 0.014; block 2, 0.022 ± 0.011; and block 3, 0.031 ± 0.016; $p < 0.05$).

There was a significant relationship between the correlations during REM and the correlations during SWS before REM

Correlations during REM were related to the correlations during block 2 ($r = 0.2 \pm 0.02$; $p < 0.0001$) and block 1 ($r = 0.16 \pm 0.02$; $p < 0.0001$); however, there was no relationship between the correlations during the REM episode and block 3, controlling for block 2 effects ($r = 0.03 \pm 0.02$; $p > 0.05$). Thus the REM episode and its associated theta activity did not appear to affect the pattern in SWS in a manner comparable with the effects of a previous waking theta episode. In two rats, three additional REM episodes were present during postbehavior sleep. In five of six of these episodes, correlations during the REM episode were related to the correlations during SWS just before the episode ($p <$ 0.05).

For the familiar condition, after a REM episode, the mean correlation in SWS increased to levels observed before REM, but there was no effect on the correlation patterns

The mean correlation of the population of cells increased in block 3 immediately after the REM episode to the block 1 value ($p >$ 0.05). However, in spite of the increase in mean correlation, the reduction in EV between blocks 1 and 3 was not substantially different from that expected from the spontaneous decay rate (Fig. 3*D*), indicating a lack of an effect of the REM episode on the memory trace for the familiar experience. There was insufficient REM data in experiment 2 for analysis.

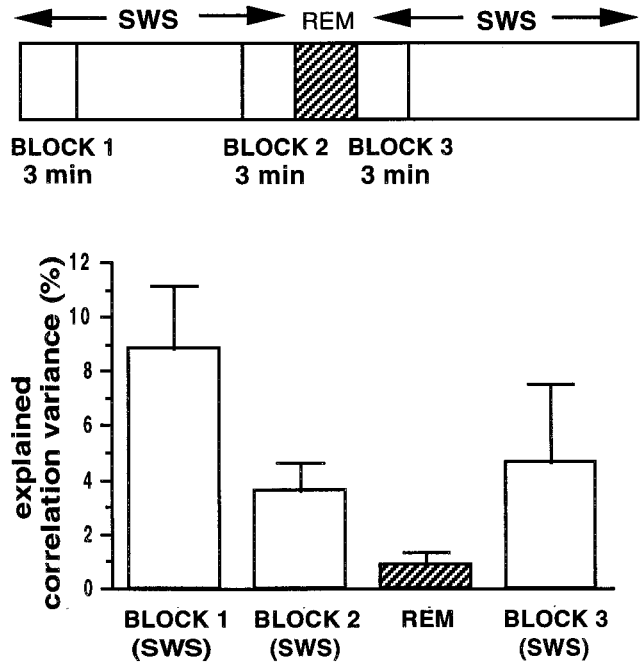

Figure 6. *Top*, Correlations were computed in POST during the first and last 3 min of a 10 min SWS period (*blocks 1*, *2*) before the first REM episode and during a 3 min period after the REM episode (*block 3*). *Bottom*, The EV during REM was significantly smaller than that in the preceding SWS (*blocks 1*, *2*; $p < 0.05$, Mann–Whitney *U* test) and was not significantly >0 ($p > 0.05$). The EV for *block 3* was significantly lower than that in *block 1* ($p < 0.05$), as expected (e.g., Fig. 3*D*). Between *blocks 2* and *3*, a decreasing trend in ripple count was observed (196 ± 15 in *block 2* compared with 133 ± 13 in *block 3*; $p < 0.05$). The firing rates during ripples showed a trend toward an increase (*block 2*, 2.06 ± 0.17 Hz; *block 3*, 2.23 ± 0.19 Hz; $p < 0.06$). During inter-ripple intervals, the firing rates showed a net decrease (*block 2*, 0.57 ± 0.05 Hz; *block 3*, 0.50 ± 0.06 Hz; $p < 0.05$).

Sleep per se is unnecessary for trace reactivation

Hippocampal EEG and population discharge characteristics in the quiet waking state are essentially indistinguishable from that of SWS, being characterized by the same sharp wave–ripple complexes and associated complex spike bursts. This raises the question of whether sleep per se is an essential prerequisite for the reexpression of preceding correlation patterns. This question was addressed in one recording session. After RUN, an experimenter sat inside the recording room and intermittently stroked the rat's fur to prevent it from falling asleep. Behaviorally, the rat was in a relatively motionless but alert state, with eyes mostly open and with LIA being observed in the EEG and audible ripple bursts on the audio monitor. In this data set (28 cells), there was a significant dependency of the RUN correlation structure on that during PRE ($r_{\mathrm{RUN-PRE}} = 0.13 \pm 0.05$; $p < 0.02$; EV = 2%) and of the POST structure on that during RUN ($r_{\mathrm{RUN-POST|PRE}} = 0.35 \pm 0.05$; $p < 0.0001$; EV = 12%). These values are comparable with the effects observed during SWS. Thus, it seems that the presence of ripples may be a sufficient condition for pattern reactivation.

DISCUSSION

This study extends our understanding of the basic characteristics of off-line reactivation of activity patterns in hippocampal neuronal ensembles (Pavlides and Winson, 1989; Wilson and McNaughton, 1994; Skaggs and McNaughton, 1996; Qin et al., 1997). An experience-specific pattern of firing correlations persists during subsequent SWS and quiet wakefulness and was shown here to be quantifiable in terms of explained (in the statistical sense) variance (EV) in the correlation structure of the ensemble during these states.

During SWS and quiet wakefulness, the hippocampus exhibits irregularly timed burst activity accompanied by SPW–ripple oscillations in the EEG. Although there is significant EV because of the preceding experience in the inter-ripple intervals, the magnitude of the EV is substantially larger during the ripple events (see also Skaggs and McNaughton, 1998). This is consistent with the idea that these events reflect convergence of the network onto "attractor" states representing stored memories (McNaughton, 1983; Chrobak and Buzsáki, 1994; Wilson and McNaughton, 1994; Shen and McNaughton, 1996); however, this conjecture requires verification from further analysis. It is possible, for example, that the reduced EV in the inter-ripple intervals reflects mostly statistical error, related to the interaction between the lower firing probabilities in these periods and the minute sample size (compared with the total number of neurons). It is also possible, however, that the reactivation occurs exclusively during ripples and that the EV during the inter-ripple intervals reflects measurement error in the detection of small ripple events. Although ripple dynamics were observed to change over the course of a sleep episode, the time course of the EV itself was somewhat more persistent on average.

The EV attributable to one experience is still present, although possibly attenuated (see Fig. 5), in SWS, even if a different experience (and hence a different activity pattern) intervenes before sleep onset. This observation is consistent with the notion that the EV reflects spontaneous retrieval of stored memory traces and not merely the persistence of recent activity such as is commonly associated with "working memory" (e.g., Fuster and Alexander, 1971; Kubota and Niki, 1971; Goldman-Rakic, 1987). It cannot be ruled out that multiple independent reverberatory traces may be maintained elsewhere in the brain and imposed on the hippocampus during SWS; however, the probable origination of the ripple events in CA3 (Buzsáki, 1986; Chrobak and Buzsáki, 1994) would weigh against this hypothesis. Moreover, significant traces of familiar experiences were occasionally detected during SWS 24 hr after the last episode, in a few cases rather robustly (EV of 30–60%). Overall, the magnitude of the PRE effects for familiar environments, although usually small, was significantly >0 and significantly larger than for novel ones. This pattern suggests that the memory traces for repeated experiences may be quite well preserved, even though they may be retrieved only sporadically during sleep occurring 24 hr or more after the last instantiation of the experience.

An interesting and somewhat unexpected finding was that, at least after highly familiar experiences, the reactivation phenomenon was present during SWS and quiet wakefulness but not during REM sleep. Unfortunately, there were insufficient REM sleep data available in experiment 2 to assess whether this pattern may change after a novel experience, and further study of this question is needed. It is possible that some reactivation does occur in REM and that the failure to detect it in terms of significant EV is a consequence of different memory retrieval dynamics in the two states (see McNaughton, 1999; Skaggs and McNaughton, 1998). For example, if the speed of playback of event sequences was higher in SWS than in REM sleep, then more of the previous states could be represented in a given period of time, possibly making the correlation structure of the ensemble during a relatively brief SWS episode more similar to that of the preceding waking epoch. There is some evidence suggesting that sequence reactivation occurs during SWS at an accelerated rate (Skaggs and McNaughton, 1996). Alternatively, the extent of memory trace retrieval during REM sleep may be affected by the relative familiarity of the experience. Recently Poe et al. (1997) have shown that the firing patterns of CA1 pyramidal cells during REM sleep are different depending on whether the cells participated in the encoding of a novel experience or only a familiar one in the previous waking period. In the latter case, the firing was both less robust and occurred preferentially at a phase of the local EEG theta rhythm 180° reversed from the peak firing phase during waking behavior. They speculated that the firing of cells related to familiar events may be actively suppressed during REM, which would explain the failure, in the present study, to detect during REM any significant EV for familiar experiences. Finally, the data were not sufficient to rule out the possibility that the lack of significant effects during REM sleep is merely a consequence of the decay of the EV during the 15–30 min of SWS that typically precedes any REM bout.

Although the EV in REM caused by the preceding waking episode was not statistically significant, there was a significant EV in REM attributable to the immediately preceding episode of SWS. We do not think that either the data or the current analytical techniques warrant any strong conclusions about the possible functional significance of this phenomenon at present.

Pavlides and Winson (1989) reported that CA1 complex spike cells exhibited increased firing rates and more bursting activity in SWS after selective exposure of the rat to their respective place fields. The current data show a rather modest (and not statistically significant) increase (14%) in firing rates between the first and second sleep epochs of cells that were spatially active during the intervening behavior on the track. The larger effects seen in the Pavlides and Winson study could be caused by the fact that their animals were confined to a small region containing the field of a cell for 10–15 min before being allowed to sleep. Thus, the reactivation during subsequent sleep was biased to cell populations that were active in the region of the environment that the rats visited. This would lead to an apparent elevation in the mean firing rates of those cells encoding this region relative to that of those cells encoding other, unvisited regions. This would be completely compatible with the present results. In general, if recent, spatially specific patterns of activity are reexpressed in sleep, then the larger the space explored during waking, the smaller will be the expected increase in mean firing rate.

Overall, our results indicate a persistent similarity in the pattern of neuronal ensemble discharge in the rat hippocampus during SWS compared with the previous waking experience, suggesting a reactivation of recent memory traces. It is possible that the hippocampal trace reactivation may contribute to a slowly developing synaptic reorganization in the neocortex, leading to a long-lasting memory. This remains to be shown empirically [see, however, recent results of Higuchi and Miyashita (1996)]. There was an unexpected lack of such reactivation during REM sleep, at least for previously familiar experiences (insufficient data were available for the novel experiences). This was surprising in view

of the emphasis that has been placed on REM sleep per se in the memory consolidation literature. Future studies should also address the possible role of REM sleep in the replay and consolidation of novel experiences as well as the possibility that later REM cycles in the same sleep session may be devoted to the more recent experience (Smith and Butler, 1982; Smith and MacNeill, 1993).

REFERENCES

Bliss TVP, Gardner-Medwin AR (1973) Long-lasting potentiation of synaptic transmission in the dentate area of the unanaesthetised rabbit following stimulation of perforant path. J Physiol (Lond) 232:357–374.

Bliss TVP, Lømo T (1973) Long-lasting potentiation of synaptic transmission in the dentate area of the anaesthetised rabbit following stimulation of perforant path. J Physiol (Lond) 232:331–356.

Bloch V, Hennevin E, Leconte P (1979) Relationship between paradoxical sleep and memory processes. In: Brain mechanisms in memory and learning: from the single neuron to man (Brazier MAB, ed), pp 329–343. New York: Raven.

Buzsáki G (1986) Hippocampal sharp waves: their origin and significance. Brain Res 398:242–252.

Buzsáki G (1989) Two-stage model of memory trace formation: a role for "noisy" brain states. Neuroscience 31:551–570.

Buzsáki G, Horváth Z, Urioste R, Hetke J, Wise K (1992) High-frequency network oscillation in the hippocampus. Science 256:1025–1027.

Chrobak JJ, Buzsáki G (1994) Selective activation of deep layer (V–VI) retrohippocampal cortical neurons during hippocampal sharp waves in the behaving rat. J Neurosci 14:6160–6170.

Fishbein W, Gutwein BW (1977) Paradoxical sleep and memory storage processes. Behav Biol 19:425–464.

Fox SE, Ranck Jr JB (1981) Electrophysiological characteristics of hippocampal complex-spike cells and theta cells. Exp Brain Res 41:399–410.

Fuster JM, Alexander GE (1971) Neuron activity related to short-term memory. Science 173:652–654.

Gerstein GL, Perkel DH (1969) Simultaneously recorded trains of action potentials: analysis and functional interpretation. Science 164:828–830.

Goldman-Rakic PS (1987) Circuitry of primate prefrontal cortex and regulation of behavior by representational memory. In: Handbook of physiology, Vol 5, The nervous system (Plum S, ed), pp 373–417. Bethesda, MD: American Physiological Society.

Gothard KM, Skaggs WE, Moore KM, McNaughton BL (1996) Binding of hippocampal CA1 neural activity to multiple reference frames in a landmark-based navigation task. J Neurosci 16:823–835.

Hebb DO (1949) The organization of behavior. New York: Wiley.

Higuchi S, Miyashita Y (1996) Formation of mnemonic neuronal responses to visual paired associates in inferotemporal cortex is impaired by perirhinal and entorhinal lesions. Proc Natl Acad Sci USA 93:739–743.

Karni A, Tanne D, Rubenstein BS, Askenasy JJ, Sagi D (1994) Dependence on REM sleep of overnight improvement of a perceptual skill. Science 265:679–682.

Kim JJ, Fanselow MS (1992) Modality-specific retrograde amnesia of fear. Science 256:675–677.

Kleinbaum DG, Kupper LL, Muller KE (1988) Applied regression analysis and other multivariable methods. Belmont, CA: Duxbury.

Kubota K, Niki H (1971) Prefrontal cortical unit activity and delayed alternation performance in monkeys. J Neurophysiol 34:337–347.

Kudrimoti HS, McNaughton BL, Barnes CA, Skaggs WE (1995) Recent experience strengthens pre-existing correlations between hippocampal neurons during sleep. Soc Neurosci Abstr 21:941.

Kudrimoti HS, Skaggs WE, Barnes CA, McNaughton BL, Gerrard JL, Suster MS, Weaver KL (1996) REM sleep and the reactivation of recent correlation patterns in hippocampal neuronal assemblies. Soc Neurosci Abstr 22:734.

Kudrimoti HS, Barnes CA, McNaughton BL (1997) Long-term persistence of experience-induced neuronal correlations in hippocampal ensembles. Soc Neurosci Abstr 23:506.

MacKinnon D, Squire LR (1989) Autobiographical memory in amnesia. Psychobiology 17:3247–3256.

Marr D (1971) Simple memory: a theory for archicortex. Philos Trans R Soc Lond [Biol] 262:23–81.

McClelland JL, McNaughton BL, O'Reilly RC (1995) Why there are complementary learning systems in the hippocampus and neocortex: insights from the successes and failures of connectionist models of learning and memory. Psychol Rev 102:419–457.

McGaugh JL, Herz MJ (1972) Memory consolidation. San Francisco: Albion.

McGrath MJ, Cohen DB (1978) REM sleep facilitation of adaptive waking behavior: a review of the literature. Psychol Bull 85:24–57.

McNaughton BL (1983) Activity dependent modulation of hippocampal synaptic efficacy: some implications for memory processes. In: The neurobiology of the hippocampus (Seifert W, ed), pp 233–251. London: Academic.

McNaughton BL (1998) The neurophysiology of reminiscence. Neurobiol Learn Mem 70:252–267.

McNaughton BL, Morris RGM (1987) Hippocampal synaptic enhancement and information storage within a distributed memory system. Trends Neurosci 10:408–415.

McNaughton BL, Douglas RM, Goddard GV (1978) Synaptic enhancement in fascia dentata: cooperativity among coactive afferents. Brain Res 157:277–293.

McNaughton BL, Barnes CA, O'Keefe J (1983a) The contributions of position, direction, and velocity to single unit activity in the hippocampus of freely-moving rats. Exp Brain Res 52:41–49.

McNaughton BL, O'Keefe J, Barnes CA (1983b) The stereotrode: a new technique for simultaneous isolation of several single units in the central nervous system from multiple unit records. J Neurosci Methods 8:391–397.

McNaughton BL, Barnes CA, Meltzer J, Sutherland RJ (1989) Hippocampal granule cells are necessary for normal spatial learning but not for spatially-selective pyramidal cell discharge. Exp Brain Res 76:485–496.

McNaughton BL, Barnes CA, Gerrard JL, Gothard K, Jung MW, Knierim JJ, Kudrimoti H, Qin Y, Skaggs WE, Suster M, Weaver KL (1996) Deciphering the hippocampal polyglot: the hippocampus as a path integration system. J Exp Biol 199:173–185.

Muller RU, Kubie JL (1987) The effects of changes in the environment on the spatial firing of hippocampal complex-spike cells. J Neurosci 7:1951–1968.

Nadel L, Moscovitch M (1997) Memory consolidation, retrograde amnesia and the hippocampal complex. Curr Opin Neurobiol 7:217–227.

Nadel L, Wilner J, Kurz EM (1985) Cognitive maps and environmental context (Balsam PD, Tomie A, eds), pp 385–406. Hillsdale, NJ: Earlbaum.

O'Keefe J (1976) Place units in the hippocampus of the freely moving rat. Exp Neurol 51:8–109.

O'Keefe J, Dostrovsky J (1971) The hippocampus as a spatial map. Preliminary evidence from unit activity in the freely-moving rat. Brain Res 34:171–175.

O'Keefe J, Nadel L (1976) The hippocampus as a cognitive map. Oxford: Clarendon.

O'Keefe J, Recce ML (1993) Phase relationship between hippocampal place units and the EEG theta rhythm. Hippocampus 3:317–330.

O'Keefe J, Speakman A (1987) Single unit activity in the rat hippocampus during a spatial memory task. Exp Brain Res 68:1–27.

Pavlides C, Winson J (1989) Influences of hippocampal place cell firing in the awake state on the activity of these cells during subsequent sleep episodes. J Neurosci 9:2907–2918.

Paxinos G, Watson C (1982) The rat brain in stereotaxic coordinates. New York: Academic.

Perkel DH, Gerstein GL, Moore GP (1967) Neuronal spike trains and stochastic point processes. II. Simultaneous spike trains. Biophys J 7:419–440.

Poe GR, Skaggs WE, Barnes CA, McNaughton BL (1997) Theta phase precession remnants in REM sleep. Soc Neurosci Abstr 23:505.

Qin Y, McNaughton BL, Skaggs WE, Barnes CA (1997) Memory reprocessing in cortico-cortical and hippocampo-cortical neuronal ensembles. Philos Trans R Soc Lond [Biol] 352:1525–1533.

Quirk GJ, Muller RU, Kubie JL (1990) The firing of hippocampal place cells in the dark depends on the rat's recent experience. J Neurosci 10:2008–2017.

Ranck Jr JB (1973) Studies on single neurons in dorsal hippocampal formation and septum in unrestrained rats. I. Behavioral correlates and firing repertoires. Exp Neurol 41:461–531.

Samsonovich A, McNaughton BL (1997) Path integration and cognitive mapping in a continuous attractor neural network model. J Neurosci 17:5900–5920.
Scoville WB, Milner B (1957) Loss of recent memory after bilateral hippocampal lesions. J Neurol Neurosurg Psychiatry 20:11–21.
Shen B, McNaughton BL (1996) Modeling the spontaneous reactivation of experience-specific hippocampal cell assembles during sleep. Hippocampus 6:685–692.
Skaggs WE, McNaughton BL (1996) Replay of neuronal firing sequences in rat hippocampus during sleep following spatial experience. Science 271:1870–1873.
Skaggs WE, McNaughton BL (1998) Neuronal ensemble dynamics in hippocampus and neocortex during sleep and waking. In: Neuronal ensembles (Eichenbaum H, Davis J, eds). New York: Wiley.
Skaggs WE, McNaughton BL, Gothard KG, Markus EJ (1993) An information theoretic approach to deciphering the hippocampal code. In: Progress in neural information processing systems, Vol 5 (Hansen SJ, Cowan JD, Giles CL, eds), pp 1030–1037. San Mateo, CA: Kauffman.
Smith C (1995) Sleep states and memory processes. Behav Brain Res 69:137–145.
Smith C, Butler S (1982) Paradoxical sleep at selective times following training is necessary for learning. Physiol Behav 29:469–473.
Smith C, MacNeill C (1993) A paradoxical sleep dependent window for memory 53–56 h after the end of avoidance training. Psychobiology 21:109–112.
Teyler TJ, Discenna P (1986) The hippocampal memory indexing theory. Behav Neurosci 100:147–154.
Treves A, Rolls ET (1994) A computational analysis of the role of the hippocampus in memory. Hippocampus 4:374–391.
Vanderwolf CH, Kramis R, Gillespie LA, Bland BH (1975) Hippocampal rhythmical slow wave activity and neocortical low voltage fast activity: relations to behavior. In: The hippocampus, Vol 2, Neurophysiology and behavior (Isaacson RL, Pribram KH, eds), pp 101–128. New York: Plenum.
Wilson MA, McNaughton BL (1993) Dynamics of the hippocampal ensemble code for space. Science 261:1055–1058.
Wilson MA, McNaughton BL (1994) Reactivation of hippocampal ensemble memories during sleep. Science 265:676–679.
Winson J (1972) Interspecies differences in the occurrence of theta. Behav Biol 7:479–487.
Ylinen A, Bragin A, Nádasdy Z, Jandó G, Szabo I, Sik A, Buzsáki G (1995) Sharp wave-associated high-frequency oscillation (200 Hz) in the intact hippocampus: network and intracellular mechanisms. J Neurosci 15:30–46.
Zola-Morgan S, Squire LR (1993) Neuroanatomy of memory [review]. Annu Rev Neurosci 16:547–563.